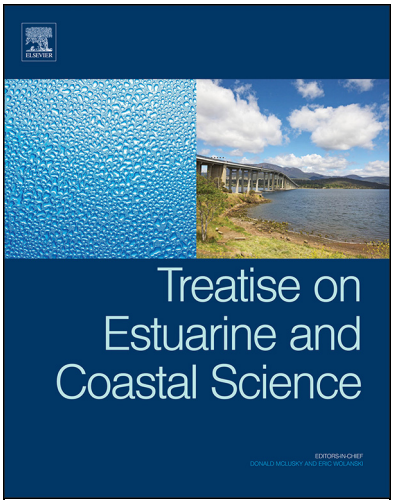

MacCready P and Banas NS (2011) Residual Circulation, Mixing, and Dispersion. In: Wolanski E and McLusky DS (eds.) *Treatise on Estuarine and Coastal Science*, Vol 2, pp. 75–89. Waltham: Academic Press.

2.05 Residual Circulation, Mixing, and Dispersion

P MacCready and NS Banas, University of Washington, Seattle, WA, USA

Abstract

This chapter covers tidally averaged circulation, salinity structure, and dispersion in estuaries. It begins with a discussion of volume and salt conservation for full estuarine systems. This leads to a focus on volume and salt fluxes through a cross section near the estuary mouth. Techniques for calculating various parts of these fluxes are reviewed, leading to the classical 'exchange' and 'tidal' parts of the up-estuary salt flux. A simple description of the physics leading to the exchange flow is given, with some discussion of the many factors ignored in its derivation. Tidal salt flux is then discussed, somewhat more informally, with comments on along-channel dispersion.

Along the way, we use specific examples from observations and numerical simulations. There is a bias toward our own work in US Pacific Northwest estuaries, but, hopefully, we have indicated some sense of the scope of work globally.

2.05.1 Introduction

Figure 1 shows examples of the observed salinity structure on along-channel sections for a variety of estuaries from around the United States. There are clear differences. We may classify some as well mixed, others as partially mixed, salt wedge, or a combination of these (Valle-Levinson, 2010). The remarkable fact, though, is how similar they are. Despite almost two orders of magnitude variation in depth, from 5 to 200 m, they exhibit common features: a more or less gradual decrease in salinity along the channel, and significant vertical stratification, as shown schematically in **Figure 2(a)**. What is not revealed by this figure is the associated circulation pattern; however, in this aspect as well, there are surprising similarities across a wide range of scales. In particular, the sub-tidal (or tidally averaged or residual) circulation in many estuaries has the form of an 'exchange flow' shown schematically in **Figure 2(b)**. This persistent current, a small residual of the often larger tidal flow, brings ocean water into the deeper part of the channel and sends less salty surface water out. Other residual circulation patterns do regularly occur – for example, lateral exchanges, complex residual eddy fields, or three- or more layer flow – and the mechanisms driving them are various, but the essential commonality of the salt fields shown in **Figure 1** indicates how central this two-layer exchange flow is to estuarine dynamics.

Exploring the physics of this exchange flow and salinity structure is the subject of the next two sections. Section 2.05.2 focuses on how the sub-tidal salt flux through any estuarine section is calculated in practice, and how it may be divided conceptually into portions associated with river flow, exchange flow, and tidal processes. The Knudsen relation is also described, providing a powerful diagnostic prediction for the exchange flow. In Section 2.05.3, the physics of the exchange flow is described, giving both classical ideas developed over 50 years ago and more recent results. The focus is on relatively narrow estuaries, in which lateral variation can be ignored to a first approximation. In Section 2.05.4, we describe some of the physical processes that lead to tidal salt flux. Often, these are tidal correlation of velocity and salinity associated with irregular topography (and here lateral variation cannot be so easily ignored). Results are summarized in Section 2.05.5, with speculation about important research questions for the future.

Estuarine residual flow and dispersion have also been reviewed extensively by other authors. In particular we recommend the excellent textbook by Fischer et al. (1979), as well as textbooks by Dyer (1977), and Lewis (1997), and review articles by Geyer and Signell (1992), Chant (2010), Monismith (2010), and MacCready and Geyer (2010).

2.05.2 Salt Balance

Estuaries are natural machines for mixing ocean and river water. Because river water is added continually, the estuary must either become fresher or export mixed water. Salinity is our primary way of distinguishing fresh river water ($s = 0$) from ocean water ($s_{ocn} \cong 30$). The export of mixed water to the coastal ocean as a river plume represents a loss of salt from the estuary and implies that ocean water must be imported if some average salinity is to be maintained, as is commonly observed (**Figure 1**). This is the essence of the exchange flow indicated schematically in **Figure 2**. Q_R is the volume flux ($m^3\ s^{-1}$) of river water. Q_{out} is the rate of export of mixed water with average salinity s_{out}, and likewise Q_{in} is the rate of import of ocean water, with average salinity $s_{in} \cong s_{ocn}$.

Salt is a dynamically active tracer, increasing the density of seawater approximately as $\rho = \rho_0(1 + \beta s)$, where $\rho_0 \cong 1000\ kg\ m^{-3}$

Treatise on Estuarine and Coastal Science, 2011, Vol.2, 75-89, DOI: 10.1016/B978-0-12-374711-2.00205-9

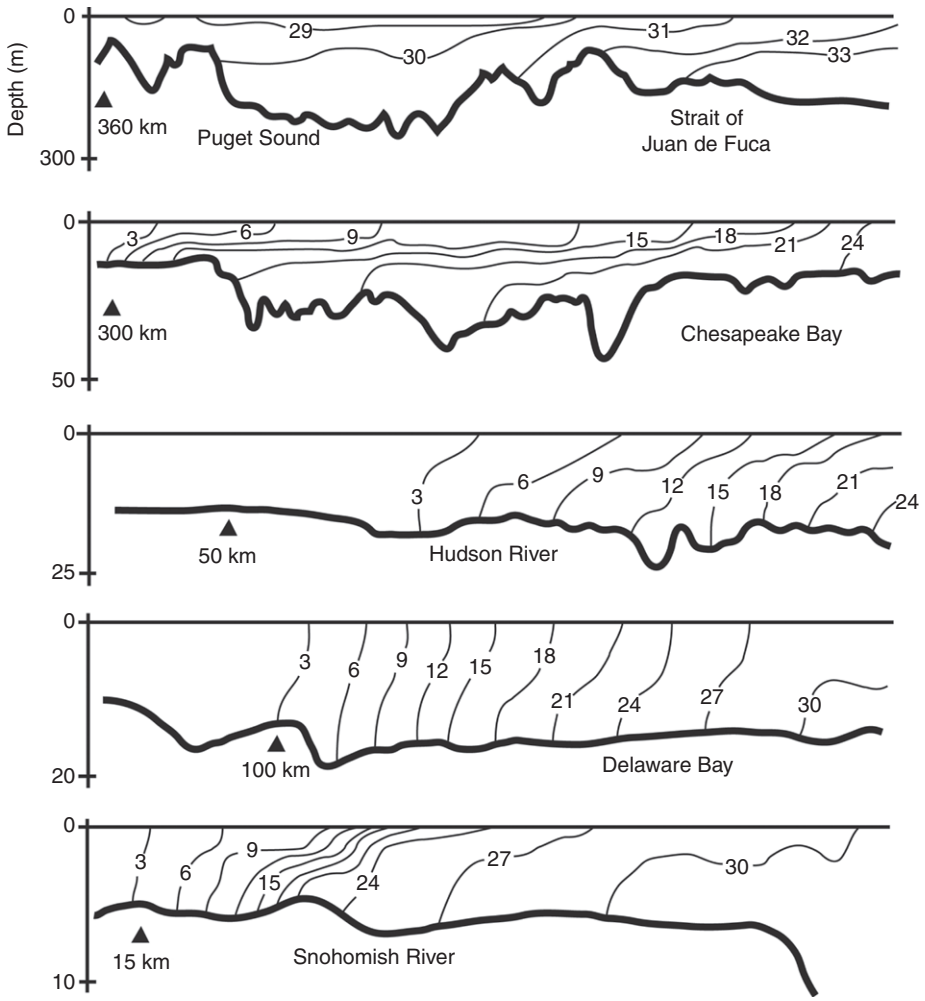

Figure 1 Along-channel salinity sections in five estuaries, highlighting the common patterns across a wide range of scales. Data are from Puget Sound, July 1953 (Collias et al., 1974); Chesapeake Bay, April 2000 (Zhang et al., 2006); Hudson River (Warner et al., 2005); Delaware Bay (Garvine et al., 1992); and Snohomish River (David Fram, personal communication). Salinity contours are labeled, and each section has different depth and length scales. In all cases, the salinity contour interval is 3, except in Puget Sound where it is 1. Notably, the stratification is weakest in Puget Sound, the deepest of the systems, a counterintuitive result of the complex interactions that control estuarine salinity structure.

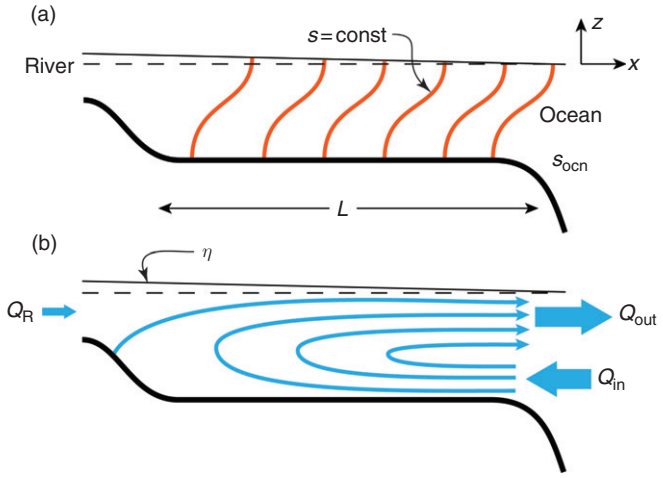

Figure 2 Sketch of idealized along-channel estuarine sections. Part (a) shows salinity contours for a partially mixed system; part (b) shows sub-tidal circulation pathways. The volume transport due to the river is Q_R, and the transports due to the exchange flow are Q_{out} and Q_{in}, defined positive in the directions drawn.

and $\beta \cong 7.7 \times 10^{-4}$. The salinity here is formally the dimensionless quantity 'practical salinity'. Physically, it is very close to the number of kilograms of salt contained in 1000 kg (~1 m^3) of seawater. The effect of salt on density is typically much greater than that of temperature; most estuaries span 25–30 of salinity and, at 16 °C, it takes a 3.5 °C temperature change to equal that of a salinity change of 1. The resulting density contrasts have profound consequences:

- The inflowing water Q_{in} tends to come in along the bottom of the estuarine channel.
- The water column maintains significant stratification, despite active tidal mixing. However, some systems such as San Francisco Bay (Stacey et al., 2001) and Liverpool Bay (Simpson et al., 1990) may become vertically well-mixed during flood tides.
- Suspended particles that sink are pulled landward, often accumulating in an 'estuarine turbidity maximum (ETM)' near the tip of the salt intrusion.
- Likewise, the organic matter produced by photosynthesis in the upper water column sinks as particles and is remineralized in the lower water column, leading to hypoxia and even anoxia there. The inward drift of the exchange flow tends to hold this water-quality problem in the landward half of the estuary (Tyler and Seliger, 1989; Mann, 2000).
- Large salinity changes are difficult for many organisms to tolerate, and estuaries tend to have lower species diversity than either fresh or marine ecosystems. However, those species that have adapted benefit from the tendency of the exchange flow to trap, hold, and recycle organic particles. Rates of primary production are very high in estuaries, often rivaling the fastest growing terrestrial ecosystems, and this is carried up the food chain (Strickland, 1983; Mann, 2000). The many large cities built on the world's estuaries found concentrated and accessible supplies of fish and shellfish.
- It is apparent that any organism that always stays near the surface is at risk of being swept to sea by the outward flux of brackish water, Q_{out}. Many marine organisms rely on the estuarine ecosystem (Able, 2005; Ray, 2005), especially during larval stages, and have developed behaviors that allow them to remain in the estuary. Other species exploit Q_{out} as larvae or juveniles to export themselves into the coastal ocean much faster than they could swim (Queiroga et al., 1994).

The size of the exchange flow was appreciated in early work on fjords by Knudsen (1900). Below, we derive the famous Knudsen relation, including the effects of time dependence. All the terms in this derivation are assumed to be tidally averaged. Later in this section, we will give much more precise definitions of how this averaging is done.

Volume conservation is governed by

$$Q_{out} = Q_R + Q_{in} \quad [1]$$

where the terms are positive in the directions shown by the arrows in **Figure 2**. This expression assumes that the total volume, V, of the estuary is not changing, usually a good approximation after averaging over tidal (or sometimes seasonal) timescales. Salt conservation, since there is no river source of salt, is given by

$$\frac{d}{dt}\int_V s\, dV = Q_{in} s_{in} - Q_{out} s_{out} \quad [2]$$

where s_{in} and s_{out} are the average salinities of the in- and outflowing water. Note that we are assuming a rather simplistic in- and outflow, with well-defined salinities. If we know these salinities and the river flow, then we may solve eqns [1] and [2] for the strength of the exchange flow, finding

$$Q_{in} = \frac{s_{out}}{\Delta s} Q_R + \frac{1}{\Delta s}\frac{d}{dt}\int_V s\, dV \quad \text{and}$$

$$Q_{out} = \frac{s_{in}}{\Delta s} Q_R + \frac{1}{\Delta s}\frac{d}{dt}\int_V s\, dV \quad [3]$$

where $\Delta s \equiv s_{in} - s_{out}$. In **Figure 1**, it is apparent that Δs is usually much less than s_{out}, and in this case the exchange flow may be many times greater than the volume flux of the river, despite the fact that the river is essential for the existence of the exchange flow. This substantial amplification underscores the fundamental importance of the exchange flow. At the mouth of Puget Sound, the amplification can be a factor of 20 (Cokelet et al., 1991; Babson et al., 2006). The result is that ocean water is being cycled through the estuary at a rapid rate.

Patterns of sub-tidal salt flux through a cross section of a real estuary are often much more complicated than the simple two-layer formalism used to derive the Knudsen relation. Currents, salinity, and even sectional area change over time and space. Any product of these that survives tidal averaging contributes to salt flux. To explore this, we use a mathematical framework developed by, for example, Fischer (1972, 1976), Hughes and Rattray (1980), Dronkers and van de Kreeke (1986), and Lerczak et al. (2006).

The sub-tidal salt flux through an estuarine cross section is given by

$$F = \langle \int us\, dA \rangle \quad [4]$$

for the section of area $A(t)$ sketched in **Figure 3**. Angle brackets denote tidal averaging. In practice, this can be done by passing a 40-h Hanning window over the time series. For signals with a significant diurnal component, the 24-24-25 Godin filter (Emery and Thomson, 1997) is more effective. When taking the area integral, we want a framework that accounts for the changing tidal height. To do this, the sectional area is divided up into a constant number of differential elements $dA(\gamma, z, t)$. The element boundaries move with time so that there are always the same number of divisions across the channel width and from the bottom to the free surface. This technique allows us to retain a plausible representation of the spatial structure of the sub-tidal flow, salinity, and salt flux. It works best when the tidal change in area is a small fraction of the total area.

Now, following Lerczak et al. (2006), we develop a way of separating the flow, salinity, and salt flux into parts which are (i) sectionally integrated or averaged and tidally averaged, (ii) sectionally varying but still tidally averaged, and (iii) a remainder that varies both over the section and over the tide. It is important to recognize that this method of averaging, and the resulting decomposition of terms, is not the only option. The

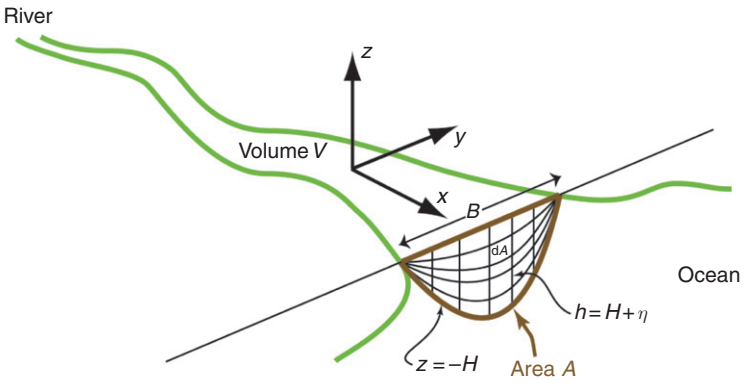

Figure 3 Schematic cross section of the estuary. The total sectional area, A, varies in time due to tidal variation of the surface height. The section is divided up into a constant number of area elements, with area dA. The elements expand and contract in time as the section width, B, and depth, h, vary with the tide.

isohaline coordinate system approach used in MacCready et al. (2002) is one alternative. It could be done in other ways, possibly leading to different, clearer, dynamical interpretations. However, the method we describe here represents the mainstream of estuarine physics and is required to understand many results in the field.

The section- and tidal-averaged terms are given by

$$A_0 \equiv \left\langle \int \mathrm{d}A \right\rangle, \quad \mathrm{d}A_0 \equiv \left\langle \mathrm{d}A \right\rangle$$
$$u_0 \equiv \frac{\left\langle \int u \, \mathrm{d}A \right\rangle}{A_0} \cong \frac{Q_\mathrm{R}}{A_0}, \quad s_0 \equiv \frac{\left\langle \int s \, \mathrm{d}A \right\rangle}{A_0} \qquad [5]$$

The term u_0 includes the Stokes drift due to correlation of velocity and surface height of progressive tidal waves. Because of this, it is a good quantity to use when making flux calculations. The sectionally varying but tidally averaged terms are defined by

$$u_1 \equiv \frac{\left\langle u \, \mathrm{d}A \right\rangle}{\mathrm{d}A_0} - u_0, \quad \mathrm{s}_1 \equiv \frac{\left\langle s \, \mathrm{d}A \right\rangle}{\mathrm{d}A_0} - s_0 \qquad [6]$$

Because of the way we allow the differential section elements to expand or contract with the tide, while always maintaining the same number of elements, the expression $\int dA$ is equivalent to a summation $\sum_{i=1}^{N} dA_i$ with the number of elements N being constant. This means that the area integrals and the time-averaging operation can be done in either order (they commute). As a result of this convenient property,

$$\int u_1 \mathrm{d}A_0 = 0, \quad \int s_1 \mathrm{d}A_0 = 0 \qquad [7]$$

The sectionally and tidally varying terms are defined as whatever is left over:

$$u_2 \equiv u - u_0 - u_1, \quad \mathrm{s}_2 \equiv s - s_0 - s_1 \qquad [8]$$

These are the high-passed (tidal) signals and have zero temporal mean, when weighted by the changing area:

$$\left\langle u_2 \, \mathrm{d}A \right\rangle = 0, \quad \left\langle s_2 \, \mathrm{d}A \right\rangle = 0 \qquad [9]$$

Now, the time-mean, section-integrated salt flux may be written as

$$F = \left\langle \int us \, \mathrm{d}A \right\rangle = \left\langle \int (u_0 + u_1 + u_2)(s_0 + s_1 + s_2) \mathrm{d}A \right\rangle$$
$$= \underset{F_\mathrm{R}}{u_0 s_0 A_0} + \underset{F_\mathrm{E}}{\int u_1 s_1 \mathrm{d}A_0} + \underset{F_T}{\left\langle \int u_2 s_2 \mathrm{d}A \right\rangle} \qquad [10]$$

The averaging properties [7] and [9] were used to eliminate six of the terms in this complicated expression. The salt flux has thus been separated into three parts, and much estuarine theory in the past half-century has tried to develop physical predictions of each term. The first term is easy to understand:

$$F_\mathrm{R} = u_0 s_0 A_0 = Q_\mathrm{R} s_0 \qquad [11]$$

is the tendency of the river flow to advect salt. This will always be a seaward salt flux, positive for x increasing toward the mouth.

The second term F_E is called the 'exchange flow' salt flux, and is built of basically the same pieces we used to make the Knudsen relation earlier in this section. Recall that u_1 and s_1 are the sectionally varying anomalies of the low-passed velocity and salinity, away from their sectional averages u_0 and s_0. If the tidally averaged circulation resembles the sketch in Figure 2, then u_1 will be positive (seaward) in the upper part of the water column, and negative below. Similarly, s_1 will be negative above and positive below for a stably stratified system. (The reader is warned that the sign convention can switch depending on how the estuary coordinate system is defined, but the directions 'up-estuary' and 'down-estuary' will always have the same meaning.) The area-integrated product of these, F_E, will then generally be negative, meaning that it moves salt up-estuary. In the next section, we explore the physics that creates these vertically varying fields. Often, the exchange flow salt flux, F_E, is nearly big enough to balance the river term, F_R, and, in this case, the Knudsen relation is an excellent approximation. From this, we may deduce that the magnitude of u_1 may be significantly greater than that of u_0, in the same way that Q_in and Q_out may be much greater than Q_R.

The final term in the salt flux is F_T, the 'tidal' term that results from primarily tidal timescale correlations of velocity and salinity. These could arise from some systematic organization of the flow due to channel cross-sectional shape, or from more chaotic processes, such as stirring by tidal eddies in complex channels. Like the exchange flow, these typically lead to up-estuary salt flux, as discussed in Section 2.05.4.

The tidally averaged salt budget integrated over the whole volume of the estuary (Figure 3) has two aspects: the storage rate of salt in the volume and the fluxes of salt through the seaward section of the volume that we have been discussing:

$$\text{Storage} = \frac{\mathrm{d}}{\mathrm{d}t}\left\langle \int_V s\,\mathrm{d}V \right\rangle = -\left\langle \int us\,\mathrm{d}A \right\rangle = -F_\mathrm{R} - F_\mathrm{E} - F_\mathrm{T} \quad [12]$$

Mathematically, this equation is derived from the Reynolds averaged salt conservation equation

$$\frac{\mathrm{D}s}{\mathrm{D}t} = \nabla\cdot\left(K_\mathrm{S}\nabla s\right) \quad [13]$$

where $\mathrm{D}/\mathrm{D}t \equiv \partial/\partial t + \mathbf{u}\cdot\nabla$ is the material derivative operator, $\mathbf{u} = (u,v,w)$ is the velocity vector, and K_S is the eddy diffusivity of salt. While vertical turbulent salt fluxes are important, the horizontal turbulent salt flux is negligible compared to advection, that is, $[us] \gg [K_\mathrm{s}\,\partial s/\partial x]$, where [ ] denotes the 'scale of' a quantity. Kundu and Cohen (2002) and MacCready et al. (2009) give details of how the volume integral of the material derivative is calculated, accounting for the irregular volume shape, moving free surface, and open ends. The result is

$$\int_V \frac{\mathrm{D}s}{\mathrm{D}t}\,\mathrm{d}V = \frac{\mathrm{d}}{\mathrm{d}t}\int_V s\,\mathrm{d}V + \int_{A_\mathrm{open}} (\mathbf{u}\cdot\hat{\mathbf{n}})s\,\mathrm{d}A \quad [14]$$

where A_open is the area of any of the open sides of the volume that the water flows through (the mouth and river ends), and $\hat{\mathbf{n}}$ is their outward unit normal. Equation [12] follows directly from application of eqn [14] to eqn [13] (ignoring turbulent fluxes) because the only nonzero advective terms are through the seaward cross-section A.

To give a specific example of how this formalism portrays an estuary's variable dynamics, we will use results from a realistic numerical simulation of the Columbia River estuary. The model setup is described in MacCready et al. (2009), and results are compared extensively with observations in Liu et al. (2009). Because it is a 'sigma coordinate' model, the grid cells naturally look like those in **Figure 3**, deforming with the changing tidal height. **Figure 4** shows an overview of the model fields from the time period considered. The Columbia River (Jay and Smith, 1990) has strong tides and river flow, forcing a dynamical system in which about half of the up-estuary salt flux can be tidal (Hughes and Rattray, 1980). Applying the salt flux averaging and decomposition described earlier to a section in the model closest to the mouth, we find the patterns plotted in **Figure 5**. The strong riverflow leads to well-defined tidally averaged estuarine circulation (left panels) and stratification (right panels). However, there is huge tidal variation of properties, evident in the unaveraged salinity values (lower right panel). Physically, we expect tidal variability of salt because the tidal currents are pushing the along-channel salinity gradient back and forth by a distance of 10–15 km. This by itself does not lead to residual salt flux because it averages out. Near the mouth, however, much of the water that exits the estuary on ebb is swept away in the coastal currents, and water of more oceanic character comes in on the subsequent flood (Stommel and Farmer, 1952;

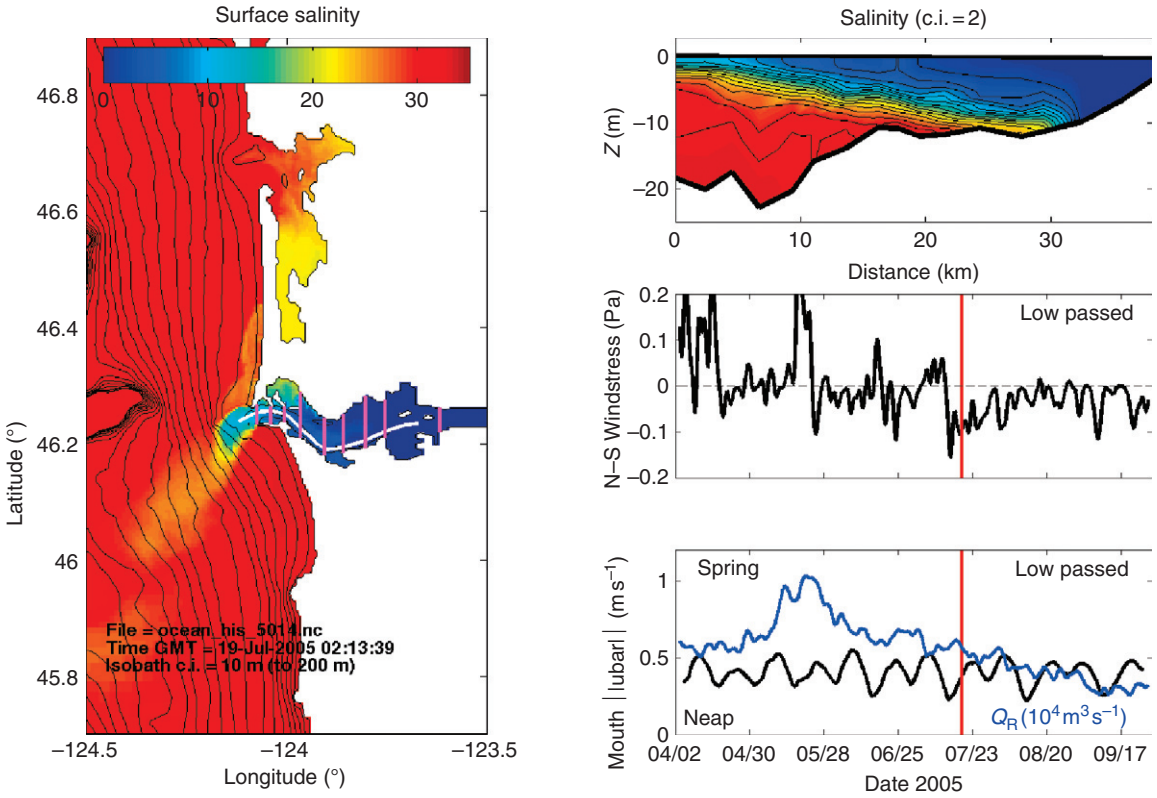

Figure 4 Fields from a realistic numerical simulation of the Columbia River estuary and plume, from 19 July 2006. A map view of surface salinity is on the left, with the path of a thalweg section through the estuary shown as a white line. The salinity on this section is plotted on the upper right. Environmental conditions at the time of this snapshot are plotted on the middle and lower right. This snapshot is at a time of moderate river flow, upwelling-favorable winds, and the transition from neap to spring tides. The black line on the lower right is the absolute value of the depth-averaged E–W current near the estuary mouth, passed through a tidal averaging filter. The magenta lines on the map show locations of the sections used to calculate salt flux terms shown in **Figures 5–7**.

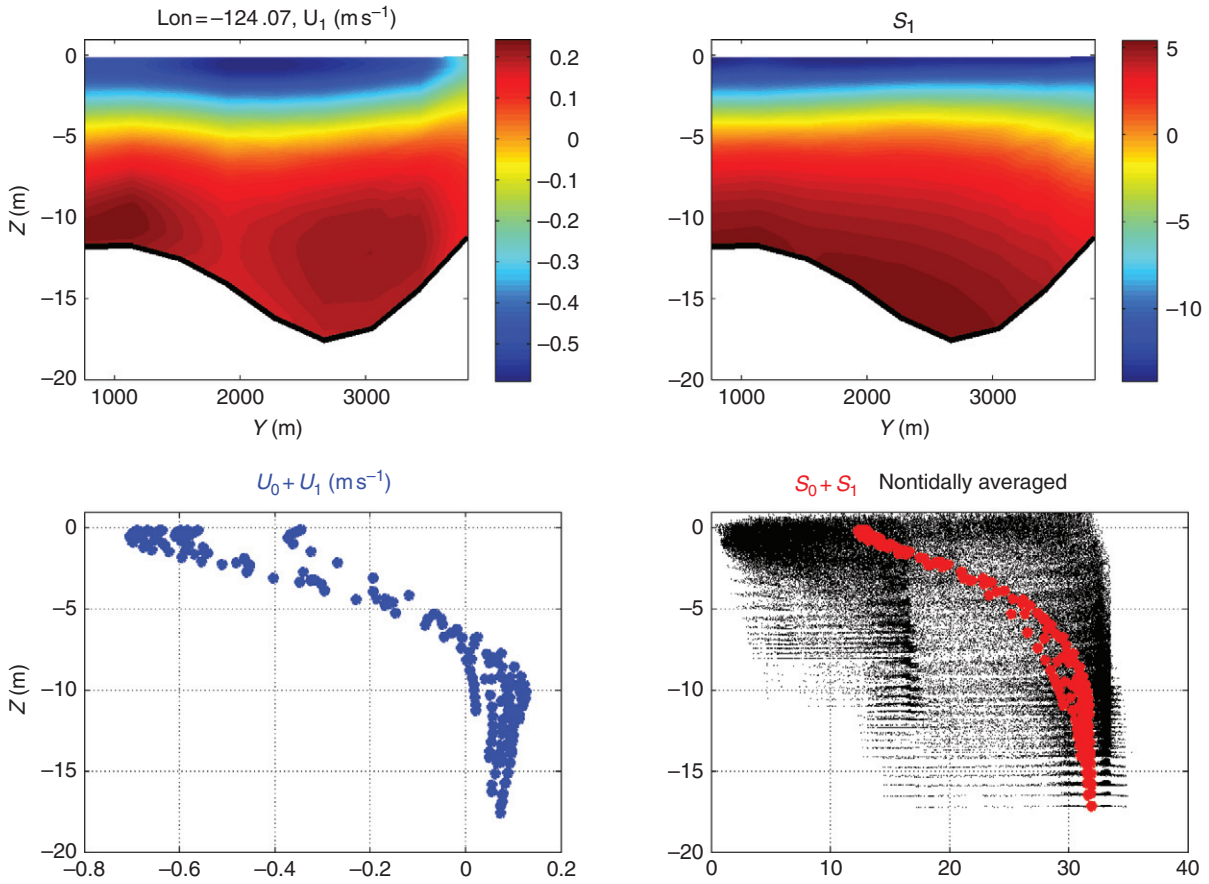

Figure 5 Tidally averaged properties from the Columbia River simulation (**Figure 4**) calculated on a section at the mouth (the leftmost magenta line in **Figure 4**). All averages are taken over a full spring–neap cycle centered on the time shown in **Figure 4**. The upper panels show the tidally averaged exchange flow, u_1, and salinity anomaly, s_1, as defined in eqns [6]. At this location, it is clear that there is a well-developed exchange flow and stratification, mostly varying in the vertical, despite the strong tidal currents. This idea is also shown by the blue and red points in the lower panels, which show all the values of $u_0 + u_1$ and $s_0 + s_1$ on this section, plotted vs. depth. Also shown on the lower right (small black points) are all the values of salinity that went into the averages, highlighting the huge tidal variability here. Caution: for the Columbia River examples, positive x and u are up-estuary, unlike the convention used elsewhere in this chapter.

Fischer et al., 1979; MacCready, 2004). The integrated flux terms as a function of along-channel position are plotted in **Figure 6** for neap tides, and in **Figure 7** for spring tides. Particularly during spring tides, and within one tidal excursion of the mouth, the up-estuary tidal salt flux dominates that due to the exchange flow. These results are consistent with what Hughes and Rattray (1980) found for this estuary analyzing the results of extensive observations.

By contrast, Lerczak et al. (2006) found exchange flow (F_E) dominance in a well-instrumented section of the Hudson. This is generally true for estuaries with stronger stratification and straight, narrow channels, such as the Hudson. Those with less stratification and wide or complex channels, such as Delaware Bay or Willapa Bay (Banas et al., 2004), can have their up-estuary salt flux dominated by F_T, and as shown above, the same is true of strongly stratified systems, such as the Columbia River, provided that the tides are especially strong (Hughes and Rattray, 1980).

Most work in the field, including our discussion so far, has viewed the storage term as a relatively small correction to what is fundamentally a steady balance between river flushing of salt and exchange flow or tidal loading of salt. However, in a system or season where riverflow is low, or variability in the ocean end member especially high, the storage term may be first order. In Willapa Bay during the summer, the low-riverflow season, the volume-integrated salt balance behaves like

$$\text{Storage} = -F_T \qquad [15]$$

Estuaries on upwelling coasts, small estuaries adjacent to large rivers, and 'tributary estuaries', such as the inner arms of the Chesapeake Bay, are also likely candidates for first-order unsteady salt balances.

2.05.3 Physics of the Gravitational Circulation

So far, we have been concerned with merely describing estuarine properties: how do we calculate tidally averaged circulation, salinity, and salt flux? We have also conceptually divided the tidally averaged salt flux into three parts: river, exchange flow, and tidal. The Knudsen relation provides a strong motivation for this analysis because it assumes that the exchange flow or

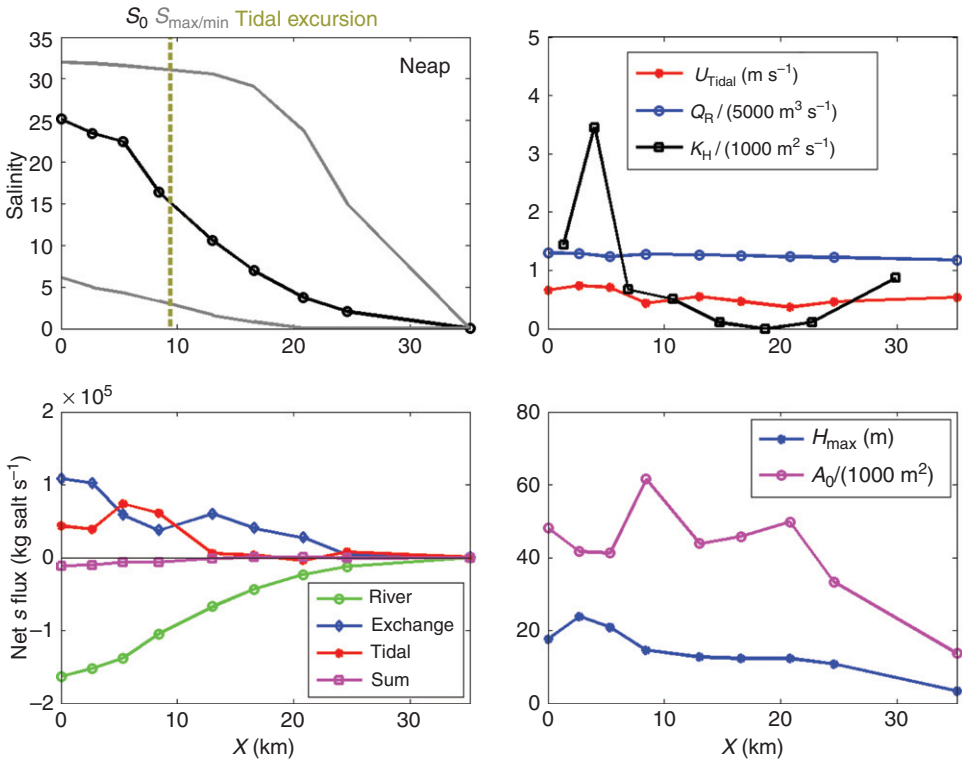

Figure 6 Terms in the salt-flux balance, averaged over a neap–tide period, at nine cross sections in the Columbia River simulation (**Figure 4**, magenta lines). The along-channel structure of the section-averaged salinity is plotted in the upper left. The gray lines show the extrema of the tidally averaged salinity (e.g., from the red points in **Figure 5**, lower right). The brown line shows one tidal excursion from the mouth. Terms in the salt balance [12] are plotted vs. along-channel position on the lower left. The 'Sum' term is the storage, and it is small, indicating that, over this neap tide, the system is in approximately steady state, but slowly losing salt. The tidal salt flux is important near the mouth. In the upper right, the river flow and amplitude of tidal velocity are plotted, along with the eddy diffusivity, K_H, required for the tidal salt flux term, as per eqn [28]. The thalweg depth and sectional area are plotted on the lower right.

overturning circulation will be a dominant feature of the sub-tidal circulation. A natural goal of estuarine physics has been to develop predictive theories for the sub-tidal circulation, stratification, and salt flux. Ideally, such theories will rely on readily available information, such as river flow, bathymetry, and the distribution of tidal currents. Here, we summarize key points of the theoretical progress of the last half-century. This section focuses on the exchange flow or 'gravitational circulation', while Section 2.05.4 focuses on tidal salt flux. Note that throughout this chapter, we often use the terms 'exchange flow' and 'gravitational circulation' interchangeably; however, this is not strictly correct. Formally, the exchange flow is the full sub-tidal exchange, for example, u_1 in the above discussion, and the gravitational circulation is only the portion of this that is forced by the pressure gradient due to the along-channel salinity gradient. As discussed later, there are other processes that may also force the exchange flow.

The first careful analysis of sub-tidal salt flux and momentum balances was done by Pritchard (1952, 1954, 1956) based on observations in the James River, a relatively narrow, partially mixed estuarine tributary of the Chesapeake. His inferences about the main dynamical balances continue to underlie estuarine theory to this day – although we will point out many improvements and challenges.

Throughout this section, we assume that the sub-tidal flow and salinity, u_1 and s_1, are mainly vertically varying, and that the estuary is a simple rectangular channel of width B and depth H. These crude simplifications allow us to make some analytical headway while retaining, we hope, the most important aspects of the physics. It follows from mass conservation that $u_0 = Q_R/A = Q_R/(HB)$. Thus, we have already succeeded in part, predicting a portion of the velocity based on the 'external' variables of river flow and bathymetry. In general, we could allow H and B to be functions of x, but for now we just assume a constant rectangular cross section. The sub-tidal surface height will be written as η_0. The surface height generally tilts downward toward the ocean. Its scale is typically a fraction of a meter, so $[\eta_0] \ll [H]$ and we may ignore it when calculating u_0.

Next, we seek a predictive equation for $u_1 = u_1(x,z,t)$. The y dependence goes away either formally through lateral averaging or less formally because the channel is narrow and we hope that lateral variation of u_1 is negligible compared to its vertical variation. The primary sub-tidal momentum balance has been assumed (Hansen and Rattray, 1965) to be one forced by the sub-tidal along-channel pressure gradient and retarded by the vertical divergence of the turbulent momentum flux:

$$0 = -\frac{1}{\rho_0}\frac{\partial\langle p\rangle}{\partial x} + \frac{\partial}{\partial z}\left\langle \tilde{K}_M \frac{\partial u}{\partial z}\right\rangle \qquad [16]$$

where p is the pressure and $\tilde{K}_M$ is the tidally varying vertical eddy viscosity. A host of terms are neglected here. Time dependence, $\partial\langle u\rangle/\partial t$, can be nonzero, but it is typically much smaller

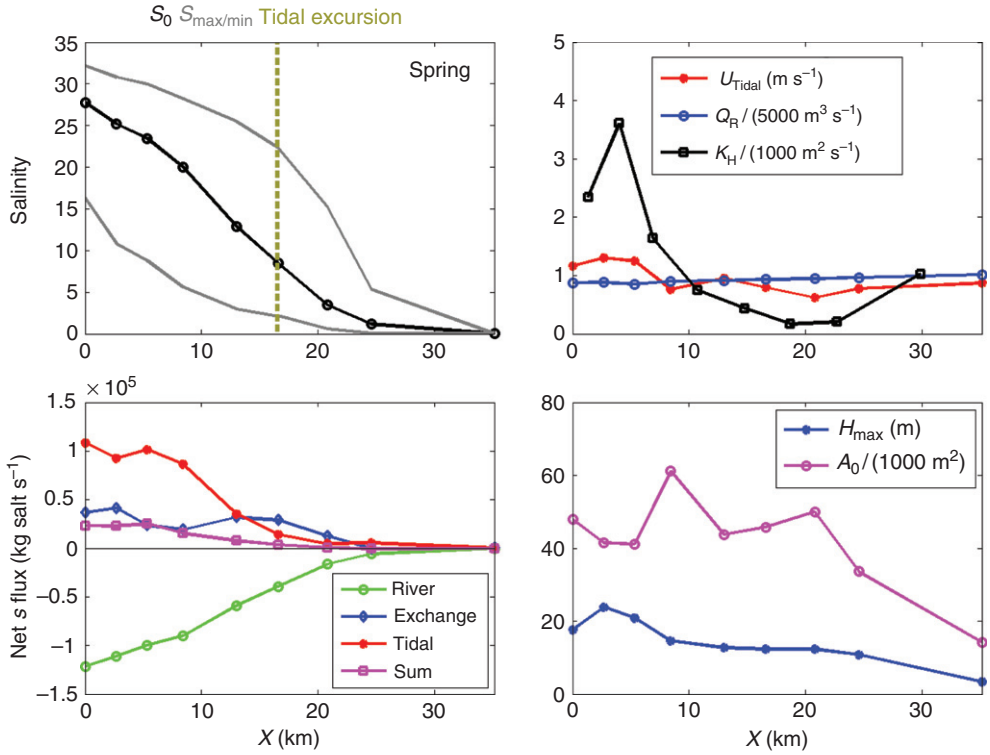

Figure 7 Same as **Figure 6**, but for a spring tide period. The estuary becomes less stratified, and the tidal salt flux term dominates over the exchange flux over most of the estuary, especially within one tidal excursion of the mouth.

than the retained terms. Momentum advection, $\langle \mathbf{u} \cdot \nabla u \rangle$, is swept under the carpet by assuming that the tidal flow is a simple back-and-forth oscillation with no spatial gradients. Caution is advisable here, though, because the tidal velocity is often an order of magnitude larger than u_1. Pritchard (1956) estimated that the modest spatial gradients of tides in the James River could make the advective term $\langle u\, \partial u/\partial x \rangle$ nonnegligible. Coriolis and the greater effect of turbulence on shallow edges of the estuarine channel may also cause leading-order modifications to the simple balance (eqn [16]), particularly in systems that are wide or weakly stratified (Valle-Levinson, 2008). There may also be considerable lateral reorganization of momentum by the cross-channel advective term $\langle v\ \partial u/\partial y \rangle$ (Lerczak and Geyer, 2004; Cheng and Valle-Levinson, 2009; Scully et al., 2009).

Finally, tidal variation of the vertical eddy viscosity, due to tidal variation of stratification, may significantly modify the frictional term, a process called 'tidal straining' (Jay and Musiak, 1994, 1996; Stacey et al., 2001). In some systems with strong tidal forcing, the tidal variation of stratification may be extreme, with complete vertical homogenization of the density at the end of flood tide. This is called 'strain-induced periodic stratification' or SIPS by Simpson et al. (1990). The decreased stratification allows stronger turbulence during flood, causing more momentum to be mixed down near the bed on that phase of the tide. The resulting tidally averaged circulation has the same sense as the gravitational circulation (landward at depth, seaward above), even though the physics is very different. In a recent numerical study, Burchard and Hetland (2010) found that in a periodically stratified one-dimensional (1-D) model, approximately two-thirds of the estuarine circulation was due to tidal straining and one-third to the gravitational circulation.

A more detailed review of recent studies of these many effects is given in MacCready and Geyer (2010). An excellent review of the fundamental equations and the approximations leading to them is given in Dyer (1997).

Now, suitably forewarned, we proceed with our analysis of the momentum balance (eqn [16]). The sub-tidal pressure gradient is hydrostatic, and can be written as the sum of contributions from the surface tilt and the underlying sub-tidal density structure:

$$-\frac{1}{\rho_0}\frac{\partial \langle p \rangle}{\partial x} \cong -g\frac{\partial \eta_0}{\partial x} - g\int_z^0 \frac{1}{\rho_0}\frac{\partial \langle \rho \rangle}{\partial x}\mathrm{d}z \cong -g\frac{\partial \eta_0}{\partial x} + g\beta\frac{\partial s_0}{\partial x}z \quad [17]$$

The integral in the second term has been evaluated assuming that $[\partial s_0/\partial x] \gg [\partial s_1/\partial x]$, meaning that the along-channel density gradient is dominated by variation of the section-averaged density, even if the system is stratified. The analytical motivation for making this approximation is that it allows us to evaluate the integral. If we also assume that the eddy viscosity is independent of depth (and that its tidal variation is unimportant), the sub-tidal momentum budget is

$$0 = -g\frac{\partial \eta_0}{\partial x} + g\beta\frac{\partial s_0}{\partial x}z + K_M\frac{\partial^2 u_1}{\partial z^2} \quad [18]$$

The necessary boundary conditions are that the flow has (1) no slip at the bottom: $(u_0 + u_1)|_{z=-H} = 0$, (2) no stress at the free surface: $\partial u_1/\partial z|_{z=0} = 0$, and (3) that it carries the river flow: $u_0 = Q_R/(HB)$. We need three conditions because [18] is a second-order equation but $\partial \eta_0/\partial x$ is also unknown. The

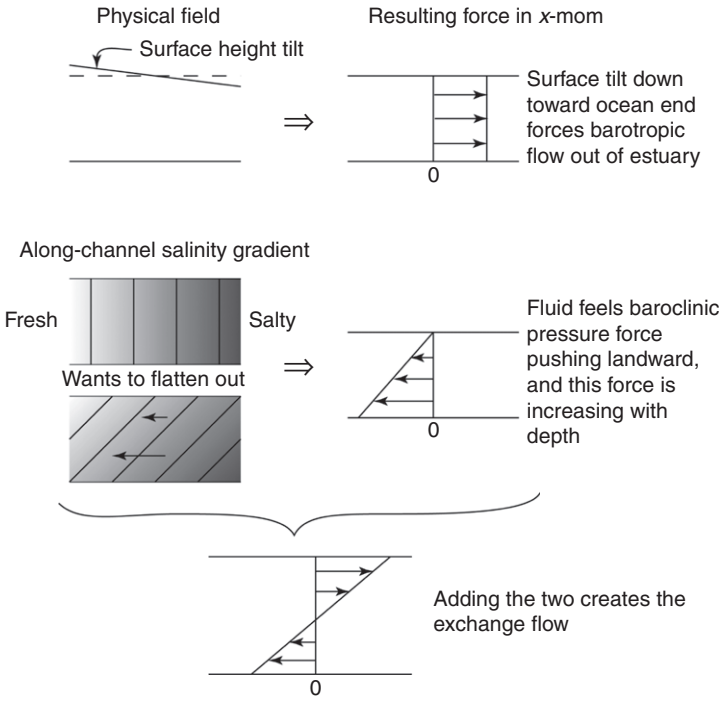

Figure 8 Schematic representation of the physics leading to the exchange flow.

solution is usually found by taking the z derivative of [18], integrating the result directly, and then applying the three conditions to find the three constants of integration. The exchange flow has zero vertical mean: $(1/H)\int_{-H}^{0} u_1\, dz = 0$. The forcing by the two pressure gradient terms is shown graphically in Figure 8. The pressure gradient due to $\partial s_0/\partial x$ only pushes water up-estuary, and this tendency increases with depth. The resulting transport increases sea level slightly at the river end, causing a competing pressure gradient, now pushing seaward and independent of depth. The sum of these adjusts rapidly to approximately equalize the inflow and outflow. Friction allows a steady balance to be achieved, and the velocity profile is the bidirectional exchange flow we have been discussing. Geyer et al. (2000), working from extensive observations in the Hudson River, showed that the actual momentum balance has some important differences from the analytical theory presented here. Mainly, the mid-depth shear stress, and with it $\partial\eta_0/\partial x$, are smaller in the observations. Nonetheless, Ralston et al. (2008) noted that the solution forms presented below can have reasonable skill. The exact functional form of the solution is a cubic polynomial, plotted in Figure 9**(b)**:

$$\langle u \rangle = u_0 + u_1 = u_0\left(\frac{3}{2} - \frac{3}{2}\zeta^2\right) + u_E\left(1 - 9\zeta^2 - 8\zeta^3\right) \qquad [19]$$

where $\zeta \equiv z/H$. The most important dynamical results are contained in the scale for the strength of the exchange flow, given by

$$u_E \equiv \frac{g\beta H^3 \partial s_0/\partial x}{48 K_M} = \frac{c^2}{48}\frac{H^2}{K_M}\frac{1}{L} \qquad [20]$$

which is close to the value of u_1 at the surface. In the expression on the right of eqn [20], we have introduced the fundamental velocity scale $c \equiv \sqrt{g\beta s_{ocn} H}$ which is proportional to the maximum speed of shallow-water, two-layer internal waves in the channel, with density contrast given by that from river to ocean water. We have also introduced L, the length of the salt

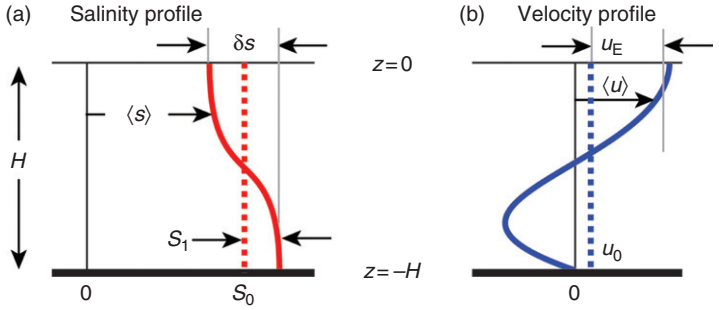

Figure 9 Sketch of terms in the exchange-flow dynamical analysis presented in Section 2.05.3. An idealized tidally, and width-averaged salinity profile is plotted in (a), and velocity profile in (b), comparable to the lower panels in **Figure 5**. The depth-averaged properties are indicated, as well as scales, δs and u_E, of the depth-varying parts.

intrusion, and assumed $\partial s_0/\partial x \approx s_{ocn}/L$. A more relevant physical interpretation of c (MacCready, 2004) is that it is close to the speed that would be attained by frictionless slumping of water due to $\partial s_0/\partial x$, over the time it takes for a water parcel to move a distance L. Thus, c represents the highest potential speed that the exchange flow could attain (in the absence of friction). This scaling gives some useful information, but the complexity of the relationship between the competing quantities $\partial s_0/\partial x$ and K_M means we have to be careful in drawing conclusions from it. Holding other terms constant, a decrease in K_M, as during neap tides, causes an increase in u_E. An early observation of this was reported in Geyer and Cannon (1982) at Admiralty Inlet, a sill at the mouth of Puget Sound. However, the term $\partial s_0/\partial x$ is part of the full solution and it may vary as well, complicating the interpretation of eqn [20]. It turns out that in shorter estuaries with strong river flow, increasing vertical turbulent mixing can shorten the salt intrusion. This has the counter-intuitive effect of making u_E insensitive to spring–neap changes in mixing (MacCready, 1999, 2007; Hetland and Geyer, 2004). This is an example of the way in which estuarine circulation and salinity structure form a closely coupled system well beyond the basic link described by the Knudsen relation [3].

Because of such complex coupling, to understand the basic functioning of an estuary, we require two more factors: predictions for the vertical stratification, and for the length of the salt intrusion (and hence $\partial s_0/\partial x$). It should be apparent from the above example why we want to predict L, and this quantity also has biological importance; but why do we want to predict the stratification? There are several answers: (1) more sub-tidal stratification can decrease turbulence, and (2) more stratified systems develop 'segregated' ecosystems, with high productivity near the surface and hypoxia and higher nutrients below. Finally, (3) the stratification is required for us to come up with a predictive theory for L, as we will see.

The main dynamical balance controlling stratification (Hansen and Rattray, 1965) can be written as

$$u_1 \frac{\partial s_0}{\partial x} = K_S \frac{\partial^2 s_1}{\partial z^2} \qquad [21]$$

In words, the exchange flow causes slumping of the along-channel salinity gradient, creating vertical stratification, as in **Figure 8**, and vertical turbulent fluxes mix the stratification away. Here, K_S is the tidally averaged vertical eddy diffusivity, again assumed constant with depth. Equation [21] is just a second-order ODE that may be integrated directly, using eqn [19] for $u_1(z)$. The result is a fifth-order polynomial, sketched in **Figure 9(a)**:

$$s_1 = \frac{H^2}{K_S}\frac{\partial s_0}{\partial x}\left[u_0\left(-\frac{7}{120}+\frac{1}{4}\zeta^2-\frac{1}{8}\zeta^4\right) + u_E\left(-\frac{1}{12}+\frac{1}{2}\zeta^2-\frac{3}{4}\zeta^4-\frac{2}{5}\zeta^5\right)\right] \qquad [22]$$

As before, the details of the derivation and solution are given by many other authors (Hansen and Rattray, 1965; Chatwin, 1976; and reviewed in MacCready and Geyer (2010)). Here, we focus on the scaling for the result. The bottom-to-top salinity difference may be shown to be

$$\delta s = s_{ocn}\frac{3}{20}\frac{u_E}{L}\frac{H^2}{K_S} \qquad [23]$$

where we have assumed $u_0 \ll u_E$. Evident in eqn [23] is the competition between the creation and destruction of stratification, expressed in terms of the ratio of two timescales: L/u_E is the time for the exchange flow to traverse the estuary, and H^2/K_S is a vertical mixing time. Notably, the terms creating stratification are quite nonlinear, increasing as $(\partial s_0/\partial x)^2$.

At this point, we have three dynamical quantities, u_E, δs, and L that describe the solution. What remains is to develop a theory for L. For the case where the 'tidal' salt flux term is negligible, this is equivalent to satisfying the Knudsen relation: the exchange term can only be big enough to balance the river term. Our volume-integrated salt budget with $F_T = 0$ is

$$\text{Storage} = -F_R - F_E \qquad [24]$$

Writing the fluxes in terms of our laterally averaged variables, and assuming steady state, we can write eqn [24] as

$$0 = -HB(u_0 s_0) - B\int_{-H}^{0}(u_1 s_1)\mathrm{d}z \qquad [25]$$

where the terms are evaluated at the mouth of the estuary; hence, $s_0 \approx s_{ocn}$. Substituting in the polynomial solutions for u_1 and s_1, one arrives at a cubic polynomial in L that may be solved to give the approximate result (Chatwin, 1976; MacCready, 1999; Monismith et al., 2002):

$$L \cong 0.024\left(\frac{c^4}{u_0}\right)^{1/3}\frac{H^2}{(K_S K_M^2)^{1/3}} \qquad [26]$$

again in the limit $u_0 \ll u_E$. The physical interpretation of eqn [26] is complicated because it involves a three-way competition of mixing, slumping, and river flow. Here, we highlight just two important aspects and suggest further reading for digging deeper.

Among the most well-observed properties is the relationship between L and u_0, with the essential prediction being that the estuary is a rather 'stiff spring', varying in length as $L \propto Q_R^{-1/3}$. The stiffness results from the fact that the ability of the exchange flow to push salt up-estuary varies as $u_E\delta s \propto L^{-3}$ and is thus very sensitive to changes in L. The theory is discussed more in MacCready (1999, 2004, 2007), Monismith et al. (2002), and Hetland and Geyer (2004). Observational evidence (for and against) is given in Abood (1974) and Ralston et al. (2008) for the Hudson, Garvine et al. (1992) for Delaware Bay, Monismith et al. (2002) for San Francisco Bay, Prandle (2009), and in Hetland and Geyer (2004) for idealized numerical experiments. Of course, many estuaries do not obey the $Q_R^{-1/3}$ scaling; notably, L in San Francisco Bay is observed to vary as $Q_R^{-1/7}$. Monismith et al. (2002) reasoned that this increased stiffness was due to feedback from the turbulence: greater river flow increases stratification, which decreases mixing. This tends to increase L in eqn [26]. Ralston et al. (2008) argued that the increased stiffness could instead be explained by the fact that the channel width and depth increase toward the mouth in San Francisco Bay, effectively making it harder to push the salt intrusion out at high river flow when it mainly occupies the deeper, wider channel.

The spring–neap variation of stratification is also quite apparent in many estuaries. It is observed in subestuaries of the Chesapeake (Haas, 1977), in Admiralty Inlet in Puget Sound (Geyer and Cannon, 1982), on the Columbia River during low flow (Jay and Smith, 1990), in the Hudson

(Lerczak et al., 2006), and in many other partially mixed systems.

In order for the stratification to vary with changing K_S, it is required that L be relatively constant. The rate at which L can vary, the so-called 'adjustment time,' has been the subject of some recent research (Kranenburg, 1986; MacCready, 1999, 2007; Hetland and Geyer, 2004; Ralston et al., 2008; Lerczak et al., 2009). The fundamental result is that the adjustment time is some fraction of the freshwater filling time:

$$T_{ADJ} \approx \frac{1}{6}\frac{L}{u_0} \qquad [27]$$

When this is comparable to or longer than the spring–neap period, then L will be relatively steady and the stratification more variable.

There are a host of important physical processes that have been glossed over in this discussion, mainly relating to the effects of lateral advection and tidal and lateral variations of mixing. These are covered in some detail in the recent review by MacCready and Geyer (2010).

2.05.4 Physics of Tidal Salt Flux and Dispersion

The remaining term in the volume-integrated salt conservation equation [12] is the 'tidal' flux F_T, the result of all correlations of transport and salinity at tidal and higher frequencies. This has often been parametrized as a Fickean diffusion, with a down-gradient salt flux proportional to the gradient of section-mean salinity (Hansen and Rattray, 1965):

$$F_T = -K_H \frac{\partial s_0}{\partial x} \qquad [28]$$

This can always be satisfied if we use the unknown horizontal dispersion parameter K_H as a fitting parameter. This was what we did in the Columbia River example shown in **Figures 6 and 7**. Because the physical mechanisms contained within K_H are diverse and often fundamentally three dimensional (B-D) and time-dependent, no comparable body of classical theory exists for K_H and F_T, as it does for exchange flow. Thus, we will only sketch possible starting points for predicting K_H in real estuaries.

K_H is frequently of the order of 100–1000 $m^2 s^{-1}$. Zimmerman (1986) described two pathways by which such a large horizontal diffusivity can arise. The first is a cascade of shear dispersion processes. Descriptions of the acceleration of tracer dispersion by either steady or oscillatory shear flow have a long history in the fluid dynamics literature, beginning with Taylor (1953) and Aris (1956) (see also Fischer et al., 1979). In Zimmerman's cascade, the dispersion associated with turbulent mixing proper (0.1–1 $m^2 s^{-1}$) is amplified by vertical shear dispersion (~10 $m^2 s^{-1}$), which is, in turn, amplified by horizontal shear (100–1000 $m^2 s^{-1}$). One factor limiting the effectiveness of oscillatory shear dispersion in many estuaries is that the timescale of cross-channel mixing is long compared to the tidal timescale (Fischer et al., 1979, Monismith, 2010).

It is common to treat the horizontal shear as a pattern of velocity gradients across a 'typical cross-section' of the estuary (an elusive concept in practice). Real and theorized estuaries frequently show a pattern of seaward flow in the deep channel balanced by landward flow on the banks (Friedrichs and Hamrick, 1996; Li and O'Donnell, 1997). However, they also frequently show the reverse pattern (Valle-Levinson and O'Donnell, 1996; Winant and Gutiérrez de Velasco, 2003), or an alternation of the two patterns along the estuary (Li, 1996; Banas and Hickey, 2005). An alternative is to schematize the horizontal shear as a field of tidal–residual eddies, as are frequently observed in the presence of channel bends (Li et al., 2006) or headlands (Signell and Geyer, 1990).

In Zimmerman's second pathway, 'Lagrangian chaos', dispersion arises from horizontal shear alone, without relying on turbulence. A steady, deterministic Eulerian residual velocity field may still be randomized by bathymetry to the point where tracers and particles disperse rapidly and chaotically. Ridderinkhof and Zimmerman (1992) demonstrated this in a model of the Wadden Sea; see also Beerens et al. (1994). This idea suggests a simple scaling for K_H, as an eddy velocity (a small fraction α of root mean square (rms) tidal velocity U_T) times an eddy width (a large fraction of the channel width B):

$$K_H = \alpha U_T B \qquad [29]$$

Banas et al. (2004) used salinity time-series data from Willapa Bay to verify that this scaling holds, with $\alpha = 0.03$–0.09. MacCready (2007) suggested replacing B with the minimum of channel width and tidal excursion distance. This latter idea accords with the result by Zimmerman (1976) that most dispersion is associated with bathymetric variation in a band of length scales around the tidal excursion scale: very large and very small bathymetric variation do not efficiently generate residual currents.

Several studies have led to a greater understanding of the physics of individual tidal eddies, and their effect on dispersion. At their simplest, tidal eddies are circulating flow structures with large potential vorticity anomaly, forced by flow separation, as the large-scale tidal current tries to go past some rough topography, such as a headland. The eddy size may be similar to the topographic scale or the tidal excursion; hence, eddies several kilometer in diameter are not uncommon. Eddy velocities may be comparable to the tidal velocity that drives them. These scales lead immediately to an appreciation of the strong impact these eddies may have on tidal dispersion: a mixing length scaling (Fischer et al., 1979) gives

$$K_H \sim L_{topo} U_T \sim 1\ \text{km} \times 0.5\ \text{m s}^{-1} = 500\ \text{m}^2\ \text{s}^{-1} \qquad [30]$$

where these scales are typical of the Three Tree Point headland discussed below. Translating this to a length scale, the usual scaling result from the diffusion equation is that a tracer patch will disperse in time as $L_{dispersion} \approx \sqrt{K_H t}$, which would be ~7 km in a day. Comparing this to the dispersive capability of the exchange flow, a typical value for u_E is 10 cm s^{-1}, which would transport a tracer ~9 km in a day. The conclusion we can reach is that, depending on the scales involved, dispersion by tidal eddies and dispersion by the exchange flow can easily be comparable. Note that there is a discrepancy (the factor $\alpha \sim 1/20$) between the scale estimates [29] and [30]. This is indicative of the uncertainty in this analysis. This arises from a fundamental lack of clarity about what scales to use, and from a lack of observations.

The physics of generation of tidal headland eddies is treated carefully in Signell and Geyer (1991) and is connected to loss of energy from the large-scale tide in Edwards et al. (2004) and

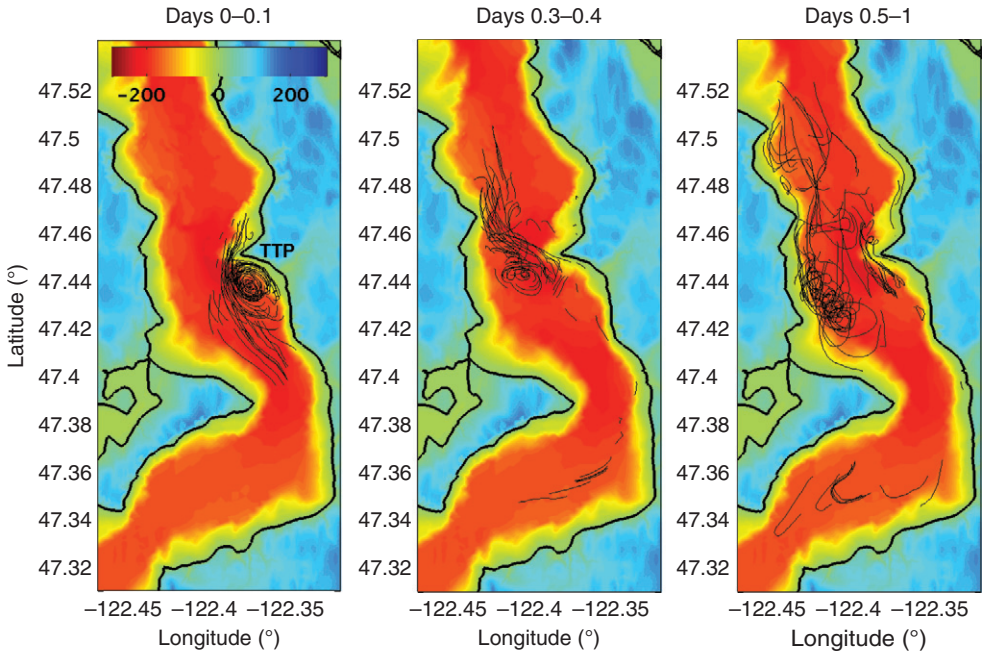

Figure 10 Horizontal dispersion due to headland eddies. The thin black lines are tracks of global positioning system (GPS)-tracked drifters deployed near the Three Tree Point headland in Puget Sound, WA. The color is depth in meters. The drifters are drogued at 20 m, and the channel is ~200 m deep here. Flood currents are southward, and the flood eddy is best resolved by these deployments. Data are from multiple days (described in McCabe et al. (2006)) and then combined using time relative to each day's maximum flood current (times shown in titles). In the left panel, the development of the flood eddy is shown. In the middle panel, we see the eddy is released from the Point and is advected across the channel. Some drifters that were not entrained in the eddy ended up very far south. In the right panel, we see that after a day, drifters, all initially deployed near the Point, are dispersed over ~18 km, although the dispersion is decidedly patchy.

Warner and MacCready (2009). In a series of numerical experiments, Signell and Geyer (1990) found that for a tidal flow with amplitude 0.5 m s^{-1} past a headland of length scale 5 km, the lateral dispersion of particles was ~10 m^2 s^{-1}. However, that result was strongly dependent on the initial location of the patch of particles, and rapid dispersion only occurred when the particle patch passed through a region of high lateral shear.

In an observational study using near-surface drifters at Three Tree Point, a 1-km headland in Puget Sound, WA, McCabe et al. (2006) mapped out the creation of a headland eddy during the flood tide (**Figure 10**). Following the drifter trajectories over a day, many processes are evident: eddy formation, advection, and decay (Pawlak et al., 2003). Drifters released near the Point had widely varying positions after a day, ending up in very patchy distributions over 18 km. This is suggestive of a scaling with numbers as in eqn [30], whereas the Signell and Geyer (1990) experiment is more consistent with eqn [29]. The difference may have to do with eddy longevity. In the Three Tree Point flow, the water is deep, 200 m, so eddy lifetimes may be long compared with the tidal period, greatly enhancing their dispersive capability.

In the Zimmerman (1986) shear dispersion cascade model, one treats the residual velocity gradients as simple and directional; in the Lagrangian chaos model, one treats them as random and isotropic; but both conceptual models are based on the idea of a tidally averaged velocity field acting on a tidally averaged tracer field. It is also possible for dispersion to arise from correlations between velocity and tracer concentration in time, over the course of the tidal cycle. These correlations (between an oscillating tidal flow and the oscillating concentration of a tracer advected by that flow) can be thought of as phase lags between the two time series, any deviation of the two time series from sinusoids in quadrature. Okubo (1973) suggested a scaling for the horizontal diffusivity associated with 'tidal trapping', in which a small amount of tracer exits the main flow into a side embayment or secondary channel at one phase of the tide and returns to the main flow after some delay. MacVean and Stacey (2010) suggested an alternate scaling based on an advective rather than diffusive conceptual model, and test it using data from breached salt ponds in south San Francisco Bay.

In practice, real estuarine bathymetry is always complicated enough that all these mechanisms occur simultaneously. A traditional strategy for attempting to differentiate them is a Reynolds-like decomposition of the net salt flux across a section into mean and varying parts in time and space (e.g., Fischer, 1976; Lewis and Lewis, 1983; Dronkers and van de Kreeke, 1986), an elaboration of what we did in eqn [10]. Unfortunately, this decomposition of terms cannot always be interpreted cleanly as a decomposition of processes; for example, it is likely that dispersion by a residual eddy field will produce a rectified salt flux that shows up in the tidally averaged shear term F_E rather than F_T, thus confusing the physical interpretation of both. Banas and Hickey (2005) demonstrated an alternate strategy using a model of Willapa Bay, in which they mapped, for each of several section lines drawn across the bay, the sets of points where a particle released at one high tide was found on the other side of the section at the next high tide. These 'crossing regions,' shown in **Figure 11**, reveal a diverse landscape of exchange processes,

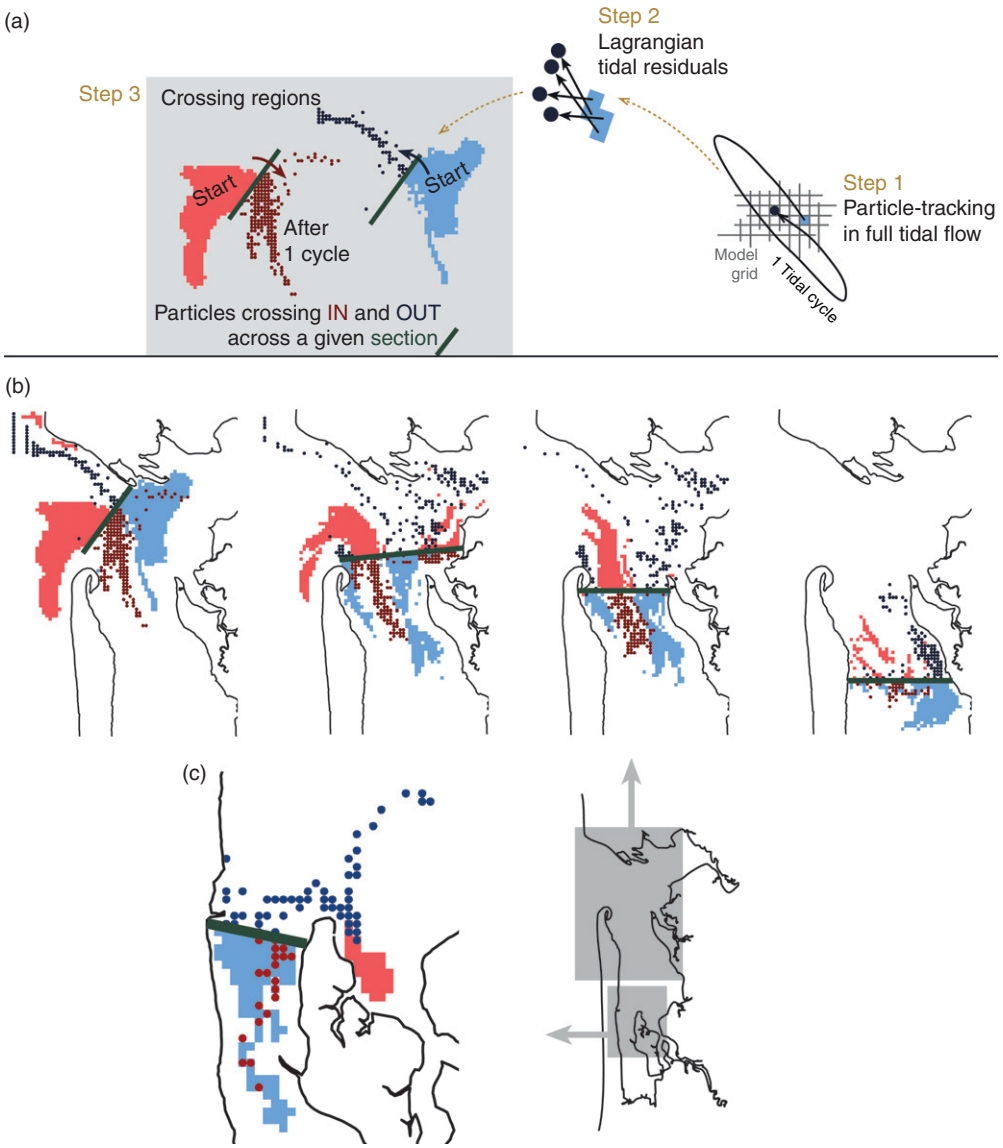

Figure 11 (a) Schematic of the method for constructing Lagrangian 'crossing regions' from numerical particle tracking in a simulation of tidal dispersion in Willapa Bay, WA. Initial particle positions are shown in light shades, and positions one tidal cycle later are shown as dark points; for a given cross section (green line), particles crossing seaward are shown in blue, and particles crossing landward are in red; particles that begin and end on the same side of the cross section are not plotted. (b, c) Crossing regions for sections near the mouth (b) and at the channel junction farther into the estuary (c). Adapted from Banas, N.S., Hickey, B.M., 2005. Mapping exchange and residence time in a model of Willapa Bay, Washington, a branching, macrotidal estuary. Journal of Geophysical Research, 110, C11011. doi:10.1029/2005JC002950.

ranging from a smooth pattern of lateral shear near the mouth, to a discontinuous, diffusion-like pattern mid-estuary, in which incoming and outgoing water masses appear to move through each other rather than past each other, to hybrid processes at channel junctions suggestive of tidal trapping. The analytically useful concept of the typical cross-section, through which one can decompose fluxes as in eqn [10] may be more stymying than helpful in such cases, where the fundamental mechanisms behind the estuary's salinity structure (such as horizontal eddies) are best understood in plan view. To make progress on a general theory of dispersion in systems like this, we probably need to start treating as fundamental the aspects of estuarine bathymetry that morphodynamicists treat as fundamental, such as channel sinuosity, dendritic patterns, and ebb-dominant/flood-dominant channel pairs (van Veen, 2002, Hibma et al., 2004).

2.05.5 Summary and Conclusions

In this chapter, we have given an overview of some of the important ideas about estuarine residual circulation and dispersion. Our discussion was framed in terms of a volume-integrated salt budget, although this is by no means the only approach to the subject. Tidally averaged salt flux through a seaward section was divided conceptually into parts associated with the river flow, the gravitational circulation, and tidal stirring. A simple theoretical framework for the

gravitational circulation was reviewed. Various mechanisms and theoretical scalings of the tidal salt flux were presented, focusing especially on the effects of complex channel shape and headland eddies.

This is by no means a thorough review of any of these topics – indeed, most have been the subjects of a dense body of research and have separate review articles or even books written about them. The point here is that real-world estuaries, such as those represented by the range in **Figure 1**, are the result of many processes going on simultaneously. In particular, our field is grappling with the effects of complex 3-D bathymetry. Indeed, depth variation is so prevalent in real estuaries that the concept of what depth to use in our parametrizations, such as eqns [20] and [23], is highly questionable. The problem is even worse when we try to assign a length scale, or any other compact metric, to the rich geomorphology of a place such as Willapa Bay. These are questions future research will confront. The culmination of this line of inquiry would be the ability to start in a new estuary with no more than a bathymetric chart, a tide gauge, a riverflow record, and predict the residual circulation and water column structure as in **Figure 1** using pencil and paper. Hopefully with better theory, more extensive observations, and the use of realistic and idealized numerical simulations, we will grow into this long-sought ability.

Acknowledgments

The authors wish to thank Rocky Geyer, Stephen Monismith, Mark Stacey, and Barbara Hickey for their many insights and discussions of these ideas over the years. PM was supported by the National Science Foundation (NSF) grant OCE 0849622. Both authors were supported by the University of Washington PRISM project.

References

Able, K.W., 2005. A re-examination of fish estuarine dependence: evidence for connectivity between estuarine and ocean habitats. Estuarine, Coastal and Shelf Science 64, 5–17.

Abood, K.A., 1974. Circulation in the Hudson River estuary. In: Roels, O.A. (Ed.), Hudson River Colloquium. Annals of the New York Academy of Sciences, New York Academy of Sciences, New York, vol. 250 pp. 38–111.

Aris, R., 1956. On the dispersion of a solute in a fluid flowing through a tube. Proceedings of the Royal Society of London A 235, 67–77.

Babson, A.L., Kawase, M., MacCready, P., 2006. Seasonal and interannual variability in the circulation of Puget Sound, Washington: a box model study. Atmosphere-Oceans 44, 29–45.

Banas, N.S., Hickey, B.M., 2005. Mapping exchange and residence time in a model of Willapa Bay, Washington, a branching, macrotidal estuary. Journal of Geophysical Research 110, C11011. doi:10.1029/2005JC002950.

Banas, N.S., Hickey, B.M., MacCready, P., Newton, J.A., 2004. Dynamics of Willapa Bay, Washington, a highly unsteady partially mixed estuary. Journal of Physical Oceanography 34, 2413–2427.

Beerens, S.P., Ridderinkhof, H., Zimmerman, J.T.F., El Naschie, M.S., 1994. An analytic study of chaotic stirring in tidal areas. In: Aref, H. (Ed.), Chaos Applied to Fluid Mixing. Pergamon, Oxford, pp. 267–285.

Burchard, H., Hetland, R.D., 2010. Quantifying the contributions of tidal straining and gravitational circulation to residual circulation in periodically stratified tidal estuaries. Journal of Physical Oceanography 40, 1243–1262.

Chant, R.J., 2010. Estuarine secondary circulation. In: Valle-Levinson, A. (Ed.), Contemporary Issues in Estuarine Physics. Cambridge University Press, Cambridge, pp. 100–124.

Chatwin, P.C., 1976. Some remarks on the maintenance of the salinity distribution in estuaries. Estuarine and Coastal Marine Science 4, 555–566.

Cheng, P., Valle-Levinson, A., 2009. Influence of lateral advection on residual currents in microtidal estuaries. Journal of Physical Oceanography 39, 3177–3190. doi:10.1175/2009JPO4252.1.

Cokelet, E.D., Stewart, R.J., Ebbesmeyer, C.C., 1991. Concentrations and ages of conservative pollutants in Puget Sound. Puget Sound Research '91. Puget Sound Water Quality Authority, Seattle, WA, vol. 1, pp. 99–108.

Collias, E.E., McGary, N., Barnes, C.A., 1974. Atlas of Physical and Chemical Properties of Puget Sound and Its Approaches. Washington Sea Grant, WSG 74-1. University of Washington Press, Seattle, WA, 235 pp.

Dronkers, J., van de Kreeke, J., 1986. Experimental determination of salt intrusion mechanisms in the Volkerak estuary. Netherlands Journal of Sea Research 20, 1–19.

Dyer, K.R., 1997. Estuaries: A Physical Introduction, Second edn. Wiley, Chichester, 195 pp.

Edwards, K.A., MacCready, P., Moum, J.N., Pawlak, G., Klymak, J., Perlin, A., 2004. Form drag and mixing due to tidal flow past a sharp point. Journal of Physical Oceanography 34, 1297–1312.

Emery,W.J., Thomson, R.E., 1997. Data Analysis Methods in Physical Oceanography. Pergamon Press, Kent, 634 pp.

Fischer H.B., 1972. Mass transport mechanisms in partially stratified estuaries. Journal of Fluid Mechanics 53, 671–687.

Fischer H.B., 1976. Mixing and dispersion in estuaries. Annual Review of Fluid Mechanics 8, 107–133.

Fischer H.B., List, E.J., Koh, R.C.Y., Imberger, J., Brooks, N.H., 1979. Mixing in Inland and Coastal Waters. Academic Press, Dera, 483 pp.

Friedrichs, C.T., Hamrick, J.M., 1996. Effects of channel geometry on cross-sectional variation in along channel velocity in partially stratified estuaries. In: Aubrey, D.G., Friedrichs, C.T. (Eds.), Buoyancy Effects on Coastal and Estuarine Dynamics, Coastal Estuarine Studies, vol. 53. American Geophysical Union, Washington, DC, pp. 283–300.

Garvine, R.W., McCarthy, R.K., Wong, K.-C., 1992. The axial salinity distribution in the Delaware Estuary and its weak response to river discharge. Estuarine, Coastal and Shelf Science 35, 157–165.

Geyer, W.R., Cannon, G.A., 1982. Sill processes related to deep water renewal in a fjord. Journal of Geophysical Research 87, 7985–7896.

Geyer, W.R., Signell, R.P., 1992. A reassessment of the role of tidal dispersion in estuaries and bays. Estuaries 15, 97–108.

Geyer, W.R., Trowbridge, J.H., Bowen, M.M., 2000. The dynamics of a partially mixed estuary. Journal of Physical Oceanography 30, 2035–2048.

Haas, L.W., 1977. The effect of the spring-neap tidal cycle on the vertical salinity structure of the James, York and Rappahannock rivers, Virginia, USA. Estuarine and Coastal Marine Science 4, 485–496.

Hansen, D.V., Rattray, M., 1965. Gravitational circulation in straits and estuaries. Journal of Marine Research 23, 104–122.

Hetland, R.D., Geyer, W.R., 2004. An idealized study of the structure of long, partially mixed estuaries. Journal of Physical Oceanography 34, 2677–2691.

Hibma, A., Schuttelaars, H.M., de Vriend, H.J., 2004. Initial formation and long-term evolution of channel-shoal patterns. Continental Shelf Research 24, 1637–1650. doi:10.1016/j.csr.2004.05.003.

Hughes, R.P., Rattray, M., 1980. Salt flux and mixing in the Columbia River Estuary. Estuarine and Coastal Marine Science 10, 479–494.

Jay, D.A., Musiak, J.D., 1994. Particle trapping in estuarine tidal flows. Journal of Geophysical Research 99, 20445–20461.

Jay, D.A., Musiak, J.D., 1996. Internal tidal asymmetry in channel flows: origins and consequences. In: Pattiaratchi, C. (Ed.), Mixing Processes in Estuaries and Coastal Seas. American Geophysical Union, Washington, DC, pp. 211–249.

Jay, D.A., Smith, J.D., 1990. Circulation, density distribution and neap–spring transitions in the Columbia River Estuary. Progress in Oceanography 25, 81–112.

Knudsen, M., 1900. Ein hydrographischer Lehrsatz. Annalen der Hydrographie und Maritimen Meteorologie 28, 316–320.

Kranenburg, C., 1986. A time scale for long-term salt intrusion in well-mixed estuaries. Journal of Physical Oceanography 16, 1329–1331.

Kundu, P.K., Cohen, I.M., 2002. Fluid Mechanics. Academic Press, San Diego, CA, 730 pp.

Lerczak, J.A., Geyer, W.R., 2004. Modeling the lateral circulation in straight, stratified estuaries. Journal of Physical Oceanography 34, 1410–1428.

Lerczak, J.A., Geyer, W.R., Chant, R.J., 2006. Mechanisms driving the time dependent salt flux in a partially stratified estuary. Journal of Physical Oceanography 36, 2296–2311.

Lerczak, J.A., Geyer, W.R., Ralston, D.K., 2009. The temporal response of the length of a partially stratified estuary to changes in river flow and tidal amplitude. Journal of Physical Oceanography 39, 915–933. doi:10.1175/2008JPO3933.1.

Lewis, R., 1997. Dispersion in Estuaries and Coastal Waters. Wiley, Chichester, 312 pp.

Lewis, R.E., Lewis, J.O., 1983. The principal factors contributing to the flux of salt in a narrow, partially stratified estuary. Estuarine and Coastal Marine Science 16, 599–626.

Li, C., 1996. Tidally Induced Residual Circulation in Estuaries with Cross Channel Bathymetry. Ph.D. Dissertation, University of Connecticut, Storrs.

Li, C., Armstrong, S., Williams, D., 2006. Residual eddies in a tidal channel. Estuaries and Coasts 29, 147–158.

Li, C., O'Donnell, J., 1997. Tidally induced residual circulation in shallow estuaries with lateral depth variation. Journal of Geophysical Research 102, 27915–27929.

Liu, Y., MacCready, P., Hickey, B.M., Dever, E.P., Kosro, P.M., Banas, N.S., 2009. Evaluation of a coastal ocean circulation model for the Columbia River plume in summer 2004. Journal of Geophysical Research 114, C00B04. doi:10.1029/2008JC004929.

MacCready, P., 1999. Estuarine adjustment to changes in river flow and tidal mixing. Journal of Physical Oceanography 29, 708–726.

MacCready, P., 2004. Toward a unified theory of tidally-averaged estuarine salinity structure. Estuaries 27, 561–570.

MacCready, P., 2007. Estuarine adjustment. Journal of Physical Oceanography 27, 2133–2145.

MacCready, P., Banas, N.S., Hickey, B.M., Dever, E.P., Liu, Y., 2009. A model study of tide- and wind-induced mixing in the Columbia River Estuary and plume. Continental Shelf Research 29, 278–291. doi:10.1016/j.csr.2008.03.015.

MacCready, P., Geyer, W.R., 2010. Advances in estuarine physics. Annual Review of Marine Science 2, 35–58. doi:10.1146/annurev-marine-120308-081015.

MacCready, P., Hetland, R.D., Geyer, W.R., 2002. Long-term isohaline salt balance in an estuary. Continental Shelf Research 22, 1591–1601.

Mann, K.H., 2000. Ecology of Coastal Waters: With Implications for Management, Second ed. Blackwell Science, Malden, MA, 406 pp.

MacVean, L.J., Stacey, M.T., 2010. Estuarine dispersion from tidal trapping: a new analytical framework. Estuaries and Coasts, doi:10.1007/s12237-010-9298-x.

McCabe, R., MacCready, P., Pawlak, G., 2006. Form drag due to flow separation at a headland. Journal of Physical Oceanography 36, 2136–2152.

Monismith, S.G., 2010. Mixing in estuaries. In: Valle-Levinson, A. (Ed.), Contemporary Issues in Estuarine Physics. Cambridge University Press, Cambridge, pp. 145–185.

Monismith, S.G., Kimmerer, W., Burau, J.R., Stacey, M.T., 2002. Structure and flow-induced variability of the subtidal salinity field in Northern San Francisco Bay. Journal of Physical Oceanography 32, 3003–3018.

Okubo, A., 1973. Effect of shoreline irregularities on streamwise dispersion in estuaries and other embayments. Netherlands Journal of Sea Research 6, 213–224.

Pawlak, G., MacCready, P., Edwards, K.A., McCabe, R., 2003. Observations on the evolution of tidal vorticity at a stratified deep water headland. Geophysical Research Letters 30, 2234. doi:10.1029/2003GL018092.

Prandle, D., 2009. Estuaries: Dynamics, Mixing, Sedimentation and Morphology. Cambridge University Press, Cambridge, 236 pp.

Pritchard, D.W., 1952. Salinity distribution and circulation in the Chesapeake Bay Estuaries system. Journal of Marine Research 11, 106–123.

Pritchard, D.W., 1954. A study of the salt balance in a coastal plain estuary. Journal of Marine Research 13, 133–144.

Pritchard, D.W., 1956. The dynamic structure of a coastal plain estuary. Journal of Marine Research 15, 33–42.

Queiroga, H., Costlow, J.D., Moreira, M.H., 1994. Larval abundance patterns of Carcinus maenas (Decapoda, Brachyura) in Canal de Mira (Ria de Aveiro, Portugal). Marine Ecology Progress Series 111, 63–72.

Ralston, D.K., Geyer, W.R., Lerczak, J.A., 2008. Subtidal salinity and velocity in the Hudson River Estuary: observations and modeling. Journal of Physical Oceanography 28, 753–770.

Ray, G.C., 2005. Connectivities of estuarine fishes to the coastal realm. Estuarine, Coastal and Shelf Science 64, 18–32.

Ridderinkhof, H., Zimmerman, J.T.F., 1992. Chaotic stirring in a tidal system. Science 258, 1107–1111.

Scully, M.E., Geyer, W.R., Lerczak J.A., 2009. The influence of lateral advection on the residual estuarine circulation: a numerical modeling study of the Hudson River estuary. Journal of Physical Oceanography 39, 107–124.

Signell, R., Geyer, W.R., 1990. Numerical simulation of tidal dispersion around a coastal headland. In: Cheng, R.T. (Ed.), Residual Currents and Long-Term Transport, Springer, New York, NY, pp. 210–222.

Signell, R.P., Geyer, W.R., 1991. Transient eddy formation around headlands. Journal of Geophysical Research 96, 2561–2575.

Simpson, J.H., Brown, J., Matthews, J., Allen, G., 1990. Tidal straining, density currents, and stirring in the control of estuarine stratification. Estuaries 13, 125–132.

Stacey, M.T., Burau, J., Monismith, S.G., 2001. Creation of residual flows in a partially stratified estuary. Journal of Geophysical Research 106, 17013–17037.

Stommel, H., Farmer, H.G., 1952. On the nature of estuarine circulation, Part I. Technical Report No. 52-88. Woods Hole Oceanographic Institute, Woods Hole, MA.

Strickland, R.M., 1983. The Fertile Fjord. Puget Sound Books, Washington Sea Grant Publication, Seattle, WA, 145 pp.

Taylor, G.T., 1953. Dispersion of soluble matter in solvent flowing slowly through a tube. Proceedings of the Royal Society of London A 219, 186–203.

Tyler, M.A., Seliger, H.H., 1989. Time scale variations of estuarine stratification parameters and impact on the food chains of the Chesapeake Bay. In: Neilson, B.J., Brubaker, J., Kuo, A. (Eds.), Estuarine Circulation. Humana Press, Clifton, NJ, pp. 201–233.

Valle-Levinson, A. (Ed.), 2010. Definition and classification of estuaries. In: Contemporary Issues in Estuarine Physics. Cambridge University Press, Cambridge, pp. 1–11.

Valle-Levinson, A., 2008. Density-driven exchange flow in terms of the Kelvin and Ekman numbers. Journal of Geophysical Research 113, C04001. doi:10.1029/2007JC00414.

Valle-Levinson, A., O'Donnell, J., 1996. Tidal interaction with buoyancy driven flow in a coastal-plain estuary. In: Aubrey, D.G., Friedrichs, C.T. (Eds.), Buoyancy Effects on Coastal and Estuarine Dynamics. American Geophysical Union, Washington, DC, pp. 265–281.

van Veen, J., 2002. Ebb and flood channel systems in the Netherlands tidal waters. Originally published as: Journal of the Royal Dutch Geographical Society 67, 303–325, 1950. (Introd., annot., transl. Bonekamp, H., Elias, E., Hibma, A., van de Kreeke, C., van Ledden, M., Roelvink, D., Schuttelaars, H., de Vriend, H., Wang, Z.-B., van der Spek, A., Stive, M., Zitman, T., Delft University Press.)

Warner, J.C., Geyer, W.R., Lerczak, J.A., 2005. Numerical modeling of an estuary: a comprehensive skill assessment. Journal of Geophysical Research C5, 2004JC002666.

Warner, S.J., MacCready, P., 2009. Dissecting the pressure field in tidal flow past a headland: when is form drag real? Journal of Physical Oceanography 39, 2971–2984.

Winant, C.D., Gutiérrez de Velasco, G., 2003. Tidal dynamics and residual circulation in a well-mixed inverse estuary. Journal of Physical Oceanography 33, 1365–1379.

Zhang, X., Roman, M., Kimmel, D., McGilliard, C., Boicourt, W., 2006. Spatial variability in plankton biomass and hydrographic variables along an axial transect in Chesapeake Bay. Journal of Geophysical Research 111, C05S11. doi:10.1029/2005JC003085.

Zimmerman, J.T.F., 1976. Mixing and flushing of tidal embayments in the western Dutch Wadden Sea, part I: distribution of salinity and calculation of mixing time scales. Netherlands Journal of Sea Research 10, 149–191.

Zimmerman, J.T.F., 1986. The tidal whirlpool: a review of horizontal dispersion by tidal and residual currents. Netherlands Journal of Sea Research 20, 133–154.

Treatise on Estuarine and Coastal Science, 2011, Vol.2, 75-89, DOI: 10.1016/B978-0-12-374711-2.00205-9